

Color superconducting quark matter core in the third family of compact stars

Sarmistha Banik and Debades Bandyopadhyay

Saha Institute of Nuclear Physics, 1/AF Bidhannagar, Kolkata 700 064, India

Abstract

We investigate first order phase transitions from β -equilibrated hadronic matter to color flavor locked quark matter in compact star interior. The hadronic phase including hyperons and Bose-Einstein condensate of K^- mesons is described by the relativistic field theoretical model with density dependent meson-baryon couplings. The early appearance of hyperons delays the onset of phase transition to higher density. In the presence of hyperons and/or K^- condensate, overall equations of state become softer resulting in smaller maximum masses than the cases without hyperons and K^- condensate. We find that maximum mass neutron stars are hybrid stars having a mixed phase of hadronic matter and color superconducting quark matter in the core. Depending on the parameter space, we also observe that there is a stable branch of superdense stars called the third family branch beyond the neutron star branch. Compact stars in the third family branch may contain pure color superconducting core and have radii smaller than those of the neutron star branch. Our results are compared with the recently measured mass-radius relationship by X-ray Multi Mirror-Newton Observatory.

I. INTRODUCTION

The theoretical investigation of mass-radius relationship of compact stars is important because those could be directly compared with measured masses and radii from various observations. Consequently, the composition and equation of state (EoS) of dense matter in neutron star interior might be probed. Recently, a lot of interest has been generated about an isolated neutron star (INS) known as RX J185635-3754 [1]. Several interesting features of this INS have emerged from various observations by Chandra X-ray observatory and Hubble Space Telescope (HST). It is one of the closest isolated neutron stars to our Sun. It provides a great opportunity to measure its radius and put important constraints on the EoS of dense matter in its core because of its relative brightness, isolated nature and above all a thermal spectrum from X-ray to optical wave lengths. Already, one group has claimed its radius is ~ 8 km or less [2]. This implies a very soft EoS including exotic forms of matter. And their prediction is the compact star might be a quark star [2]. On the other hand, the analysis of HST data on that compact star indicated a radius $R=11.4 \pm 2$ km and a mass $M=1.7 \pm 0.4M_{solar}$ which may be explained by many EoS including hyperons

and antikaon condensate [3]. Recently three strong spectral lines in the spectra of 28 bursts of low mass X-ray binary EXO0748-676 have been observed by X-ray Multi Mirror-Newton Observatory. The estimated gravitational red shift from those lines is $z = 0.35$ [4]. This provides us with many important informations about the structure of compact star because the gravitational redshift depends on the mass-radius ratio of a compact star.

The composition and structure of compact stars depend on the nature of strong interaction. Neutron star matter encompasses a wide range of densities- the density of iron nucleus at the surface to several times normal nuclear matter density in the core. Different phases of exotic matter with large strangeness fraction such as hyperon matter [5], Bose-Einstein condensates of strange mesons [6–13] and quark matter [5,7,14,15] may occur in neutron star interior. It was extensively investigated how the appearance of various forms of exotic matter influences the EoS and mass-radius relationship of compact stars. It is now well understood that each exotic component of matter makes the EoS soft. It was found in theoretical investigations [16] that a soft EoS generally gave rise to a compact star with smaller maximum mass and radius than those of a stiffer EoS.

A transition from hadronic matter to deconfined strange quark matter is a possibility in neutron star interior. Earlier, the quark phase was described by the MIT bag model [5,14] in the hadron-quark phase transition. The recent development in dense matter physics points to the fact that the quark matter may be a color superconductor [17–23]. In this case, quarks near their Fermi surfaces form Cooper pairs because quark-quark interaction is attractive in the antisymmetric color channel. The formation of diquark condensates breaks the color gauge symmetry. It was shown that at very high density quarks with all three flavors and all three colors might pair up so as to produce an energetically favored state called the color-flavor-locked (CFL) phase [24]. The color neutrality constraint is to be imposed in the CFL quark matter because a macroscopic chunk of quark matter must be color singlet [25,26]. Consequently, the CFL quark matter is charge neutral. Color and charge neutrality in the CFL quark matter require a non-zero value for the color chemical potential and electron chemical potential $\mu_e = 0$ respectively [25,26]. As the CFL condensate breaks chiral symmetry, the lightest degrees of freedom in this phase are Nambu-Goldstone bosons [24,27,28]. It was shown by various groups how the symmetric CFL phase behaves under stresses such as non-zero strange quark mass and electron chemical potential [27,28]. The CFL phase could relax under those stresses forming meson condensation. One such possibility is K^0 condensation in the charge neutral CFL quark matter [27]. Recently, nuclear matter-CFL quark matter phase transition [29] and its impact on the structure of compact stars have been studied [30]. Also, the structure of compact star including pure CFL quark matter has been studied by others [31].

Many interesting things may happen if one form of exotic matter sets in before the other. The early appearance of hyperons was found to delay the hadron-unpaired quark matter phase transition or vice-versa [7]. Similar effects of hyperons on the threshold of K^- condensation in hadronic matter was observed by various groups [7,10–13]. In this paper, we investigate how the formation of hyperons and antikaon condensate in the hadronic matter influences the phase transition from hadronic matter to CFL quark matter including K^0 condensate and the structure of compact stars. The paper is organised in the following way. In Sec. II, we describe the DDRH model for hadronic phase and CFL quark matter. Results of our calculation are explained in Sec. III. And Sec. IV provides a summary and

conclusions.

II. FORMALISM

Here, we discuss a phase transition from hadronic matter to CFL quark matter in compact stars. The hadronic phase is described within the framework of a Density Dependent Relativistic Hadron (DDRH) model [13,32,33]. In the DDRH model, many body correlations are taken into account by density dependent meson-baryon couplings. The hadronic phase is composed of all species of the baryon octet, (anti)kaons, electrons and muons. Therefore, the total Lagrangian density in the hadronic phase is written as $\mathcal{L} = \mathcal{L}_B + \mathcal{L}_K + \mathcal{L}_l$. In DDRH model, baryon-baryon interaction is given by the Lagrangian density (\mathcal{L}_B) [33],

$$\begin{aligned} \mathcal{L}_B = & \sum_B \bar{\Psi}_B \left(i\gamma_\mu \partial^\mu - m_B + g_{\sigma B} \sigma - g_{\omega B} \gamma_\mu \omega^\mu - \frac{1}{2} g_{\rho B} \gamma_\mu \boldsymbol{\tau}_B \cdot \boldsymbol{\rho}^\mu + \frac{1}{2} g_{\delta B} \boldsymbol{\tau}_B \cdot \boldsymbol{\delta} \right) \Psi_B \\ & + \frac{1}{2} \left(\partial_\mu \sigma \partial^\mu \sigma - m_\sigma^2 \sigma^2 \right) + \frac{1}{2} \left(\partial_\mu \delta \partial^\mu \delta - m_\delta^2 \delta^2 \right) - \frac{1}{4} \omega_{\mu\nu} \omega^{\mu\nu} \\ & + \frac{1}{2} m_\omega^2 \omega_\mu \omega^\mu - \frac{1}{4} \boldsymbol{\rho}_{\mu\nu} \cdot \boldsymbol{\rho}^{\mu\nu} + \frac{1}{2} m_\rho^2 \boldsymbol{\rho}_\mu \cdot \boldsymbol{\rho}^\mu. \end{aligned} \quad (1)$$

The field strength tensors for vector mesons are given by

$$\begin{aligned} \omega^{\mu\nu} &= \partial^\mu \omega^\nu - \partial^\nu \omega^\mu, \\ \boldsymbol{\rho}^{\mu\nu} &= \partial^\mu \boldsymbol{\rho}^\nu - \partial^\nu \boldsymbol{\rho}^\mu. \end{aligned} \quad (2)$$

Here Ψ_B denotes the isospin multiplets for baryons and the sum goes over baryon multiplets $B = N, \Lambda, \Sigma, \Xi$ and $\boldsymbol{\tau}_B$ is isospin operator. The interactions among baryons are mediated by the exchange of σ, ω, ρ and δ mesons. Here meson-baryon vertices $g_{\alpha B}(\hat{\rho})$, where α denotes σ, ω, ρ and δ fields, are dependent on vector density and adjusted to the Dirac-Brueckner-Hartree-Fock (DBHF) calculations [32,33]. The density operator $\hat{\rho}$ has the form, $\hat{\rho} = \sqrt{\hat{j}_\mu \hat{j}^\mu}$, where $\hat{j}_\mu = \bar{\Psi} \gamma_\mu \Psi$. As vertices $g_{\alpha B S}$ are Lorentz scalar functional of baryon field operators, the variation of \mathcal{L} with respect to $\bar{\Psi}_B$ gives,

$$\frac{\delta \mathcal{L}}{\delta \bar{\Psi}_B} = \frac{\partial \mathcal{L}}{\partial \bar{\Psi}_B} + \frac{\partial \mathcal{L}}{\partial \hat{\rho}_B} \frac{\delta \hat{\rho}_B}{\delta \bar{\Psi}_B}. \quad (3)$$

The rearrangement term $\Sigma^{\mu(r)} = \sum_B \frac{\partial \mathcal{L}}{\partial \hat{\rho}_B} \frac{\delta \hat{\rho}_B}{\delta \bar{\Psi}_B}$ which originates from the second term of Eq. 3, introduces additional contribution to vector self-energy [32–35].

The Lagrangian density for (anti)kaon condensation in the minimal coupling scheme [9,13] is,

$$\mathcal{L}_K = D_\mu^* \bar{K} D^\mu K - m_K^{*2} \bar{K} K, \quad (4)$$

where the covariant derivative $D_\mu = \partial_\mu + ig_{\omega K} \omega_\mu + ig_{\rho K} \boldsymbol{\tau}_K \cdot \boldsymbol{\rho}_\mu / 2$. The isospin doublet for kaons is $K \equiv (K^+, K^0)$ and that for antikaons is $\bar{K} \equiv (K^-, \bar{K}^0)$. The dispersion relation representing the in-medium energies of K^- meson for s -wave ($\mathbf{k} = 0$) condensation is given by

$$\omega_{K^-} = m_K^* - g_{\omega K} \omega_0 - \frac{1}{2} g_{\rho K} \rho_{03} , \quad (5)$$

where the effective mass of (anti)kaons in this minimal coupling scheme is given by

$$m_K^* = m_K - g_{\sigma K} \sigma + \frac{1}{2} g_{\delta K} \delta . \quad (6)$$

Here, we perform our calculation in the mean field approximation. The mean meson fields are denoted by σ , ω_0 , ρ_{03} and δ . Unlike meson-baryon couplings, meson-(anti)kaon coupling constants are density-independent here. The density of K^- mesons in the condensate state is given by

$$n_{K^-} = 2 \left(\omega_{K^-} + g_{\omega K} \omega_0 + \frac{1}{2} g_{\rho K} \rho_{03} \right) \bar{K} K = 2m_K^* \bar{K} K . \quad (7)$$

The Lagrangian density for leptons is

$$\mathcal{L}_l = \sum_l \bar{\psi}_l (i\gamma_\mu \partial^\mu - m_l) \psi_l , \quad (8)$$

where ψ_l ($l \equiv e, \mu$) is lepton spinor.

The meson field equations in the hadronic (h) phase are given by

$$m_\sigma^2 \sigma = \sum_b g_{\sigma b} n_b^{h,s} + g_{\sigma K} n_{K^-} , \quad (9)$$

$$m_\omega^2 \omega_0 = \sum_b g_{\omega b} n_b^h - g_{\omega K} n_{K^-} , \quad (10)$$

$$m_\rho^2 \rho_{03} = \frac{1}{2} \sum_b g_{\rho b} \tau_{3b} n_b^h - \frac{1}{2} g_{\rho K} n_{K^-} , \quad (11)$$

$$m_\delta^2 \delta = \frac{1}{2} \sum_b g_{\delta b} \tau_{3b} n_b^{h,s} - \frac{1}{2} g_{\delta K} n_{K^-} , \quad (12)$$

where τ_{3b} is the isospin projection of baryon $b = n, p, \Lambda, \Sigma^-, \Sigma^0, \Sigma^+, \Xi^-, \Xi^0$ and scalar and vector densities of baryon b in the hadronic phase are

$$\begin{aligned} n_b^{h,s} &= \langle \bar{\psi}_b \psi_b \rangle = \frac{2J_b + 1}{2\pi^2} \int_0^{k_{F_b}} \frac{m_b^*}{(k^2 + m_b^{*2})^{1/2}} k^2 dk \\ &= \frac{m_b^*}{2\pi^2} \left[k_{F_b} \sqrt{k_{F_b}^2 + m_b^{*2}} - m_b^{*2} \ln \frac{k_{F_b} + \sqrt{k_{F_b}^2 + m_b^{*2}}}{m_b^*} \right] , \end{aligned} \quad (13)$$

$$n_b^h = \langle \bar{\psi}_b \gamma_0 \psi_b \rangle = \frac{k_{F_b}^3}{3\pi^2} . \quad (14)$$

Here J_b is the spin projection of baryon b . The effective baryon mass is defined as $m_b^* = m_b - \Sigma_{b,h}^s$, where the expression for scalar self-energy for baryon b is

$$\Sigma_{b,h}^s = g_{\sigma b} \sigma + \frac{1}{2} g_{\delta b} \tau_{3b} \delta . \quad (15)$$

The bulk hadronic phase is charge neutral and the condition of β -equilibrium is maintained there. Chemical equilibrium condition under weak interactions is

$$\mu_i = b_i \mu_n - q_i \mu_e , \quad (16)$$

where b_i and q_i are the baryon number and charge of i th baryon and μ_n and μ_e are the chemical potentials of neutron and electron, respectively. The chemical potential of baryon b in the hadronic phase is expressed as

$$\mu_b = \sqrt{k_{F_b}^2 + m_b^*{}^2} + \Sigma_{b,h}^{0(0)} + \Sigma_h^{0(r)} , \quad (17)$$

where the usual vector self energy is

$$\Sigma_{b,h}^{0(0)} = g_{\omega b} \omega_0 + \frac{1}{2} g_{\rho b} \tau_{3b} \rho_{03} . \quad (18)$$

and the rearrangement contribution is [32]

$$\Sigma_h^{0(r)} = \sum_b \left[-\frac{\partial g_{\sigma b}}{\partial \rho_b} \sigma n_b^{h,s} + \frac{\partial g_{\omega b}}{\partial \rho_b} \omega_0 n_b^h + \frac{1}{2} \frac{\partial g_{\rho b}}{\partial \rho_b} \tau_{3b} \rho_{03} n_b^h - \frac{1}{2} \frac{\partial g_{\delta b}}{\partial \rho_b} \tau_{3b} \delta n_b^{h,s} \right] . \quad (19)$$

The above equation (16) implies that there are two independent chemical potentials μ_n and μ_e corresponding to two conserved charges i.e. baryon number and electric charge. In neutron stars, electrons are converted to muons by $e^- \rightarrow \mu^- + \bar{\nu}_\mu + \nu_e$ when the electron chemical potential becomes equal to muon mass. Therefore, we have $\mu_e = \mu_\mu$ in compact stars. Strangeness changing weak processes such as $n \rightleftharpoons p + K^-$ and $e^- \rightleftharpoons K^- + \nu_e$ may also occur in neutron star interior. From these relations, we obtain the condition of K^- condensation,

$$\mu_n - \mu_p = \mu_{K^-} = \mu_e . \quad (20)$$

The charge neutrality condition is

$$Q^h = \sum_b q_b n_b^h - n_{K^-} - n_e - n_\mu = 0, \quad (21)$$

where q_b and n_b^h are electric charge and the number density of baryon b in the pure hadronic phase, respectively and n_{K^-} , n_e and n_μ are number densities of K^- , electrons and muons respectively.

The energy density (ε^h) is related to the pressure (P^h) in the hadronic phase through the Gibbs-Duhem relation

$$P^h = \sum_i \mu_i n_i - \varepsilon^h . \quad (22)$$

Here μ_i and n_i are chemical potential and number density for i -th species. The expression of energy density in the hadronic phase is [13]

$$\begin{aligned} \varepsilon^h &= \frac{1}{2} m_\sigma^2 \sigma^2 + \frac{1}{2} m_\omega^2 \omega_0^2 + \frac{1}{2} m_\rho^2 \rho_{03}^2 + \frac{1}{2} m_\delta^2 \delta^2 \\ &+ \sum_b \frac{2J_b + 1}{2\pi^2} \int_0^{k_{F_b}} (k^2 + m_b^*{}^2)^{1/2} k^2 dk + \sum_l \frac{1}{\pi^2} \int_0^{k_{F_l}} (k^2 + m_l^2)^{1/2} k^2 dk \\ &+ m_K^* n_{K^-} . \end{aligned} \quad (23)$$

The rearrangement term does not contribute to the energy density explicitly, whereas it occurs in the pressure through baryon chemical potential. It is the rearrangement term that accounts for the energy-momentum conservation and thermodynamic consistency of the system [35].

The pure CFL quark matter is composed of paired quarks of all flavors and colors and neutral kaons which are Goldstone bosons arising due to the breaking of chiral symmetry in the CFL phase. The thermodynamic potential for electric and color charge neutral CFL quark matter to order Δ^2 is given by [24,29,30]

$$\Omega_{CFL}^q = \frac{6}{\pi^2} \int_0^\nu p^2(p - \mu)dp + \frac{3}{\pi^2} \int_0^\nu p^2(\sqrt{p^2 + m_s^2} - \mu)dp - \frac{3\Delta^2\mu^2}{\pi^2} + B, \quad (24)$$

where Δ is the color superconducting gap and B is the bag contribution. The first two terms of Eq. (24) give the thermodynamic potential of (fictional) unpaired quark matter in which all quarks that are going to pair have a common Fermi momentum ν which minimizes the thermodynamic potential of the fictional unpaired quark matter [24,29,30]. The third term is the contribution of the CFL condensate to Ω_{CFL}^q . The common Fermi momentum is

$$\nu = 2\mu - \sqrt{\mu^2 + \frac{m_s^2}{3}}, \quad (25)$$

where μ is the average quark chemical potential and m_s is the strange quark mass. Studying the pairing ansatz in the CFL phase, it was shown by various authors [26] that

$$n_u = n_r, \quad n_d = n_g \quad \text{and} \quad n_s = n_b, \quad (26)$$

where n_r, n_g, n_b and n_u, n_d, n_s are color and flavor number densities respectively. It follows from the above relation that color neutrality automatically enforces electric charge neutrality in the CFL phase. The quark number densities are $n_u = n_d = n_s = (\nu^3 + 2\Delta^2\mu)/\pi^2$. As the color neutral CFL quark matter is electric charge neutral, the corresponding electric charge chemical potential is $\mu_e = 0$. Similarly, the color chemical potential corresponding to color charge T_3 is $\mu_3 = 0$. However, the color chemical potential for color charge T_8 is $\mu_8 \neq 0$ to maintain color charge neutrality in the CFL phase [25,26].

Meson condensation may be a possibility in the CFL phase because strange quark mass introduces stress in this phase. It was argued that K^0 condensation could be formed in the cold and charge neutral CFL phase [27]. The thermodynamic potential due to K^0 condensate is [27]

$$\Omega_{CFL}^{K^0} = -\frac{1}{2} f_\pi^2 \frac{m_s^2}{4\mu^2} \left(1 - \frac{4\mu^2 m_{K^0}^2}{m_s^4}\right)^2, \quad (27)$$

where kaon mass [27]

$$m_{K^0}^2 = \frac{3\Delta^2}{\pi^2 f_\pi^2} m_u (m_d + m_s). \quad (28)$$

Here f_π is the pion decay constant [27] and m_u and m_d are up and down quark mass respectively. Here, K^0 condensation occurs when $m_s^2/2\mu \geq m_{K^0}$. The pressure in the CFL

phase including K^0 condensate is given by $P^q = -\Omega_{CFL}^q - \Omega_{CFL}^{K^0}$. The energy density (ϵ^q) is obtained from the Gibbs-Duhem relation [36].

We now describe the mixed phase of the above mentioned two phases because the phase transition from hadronic to CFL quark matter is a first order phase transition. Earlier the mixed phase of hadron and unpaired quark matter was studied by various authors [5,15,37]. In this case, baryon number and electric charge are two conserved charges in individual bulk phase. Glendenning argued conserved charges may be shared by two phases in equilibrium in the coexistence phase and the mixed phase is to be determined by Gibbs conditions along with global baryon and electric charge conservation laws [37]. It was found that the net positive charge of the hadronic phase was neutralised by the net negative charge of the unpaired quark matter in the mixed phase. Unlike unpaired quark matter, electric charge is not present in the CFL quark matter and baryon and color charge are conserved quantities here. Recently, the mixed phase of nuclear matter and CFL quark matter including Goldstone bosons π^- or K^- has been constructed using Glendenning's prescription [29,30]. It has been shown that K^- or π^- condensate is formed at the cost of electrons of the hadronic phase and makes the CFL phase negatively charged in the mixed phase. As color charge in the bulk hadronic phase and electric charge in the bulk CFL phase can not be present, we relax the global conservation laws of Glendenning's [37] and consider only local electric charge neutrality in the hadronic phase and local color charge neutrality in the CFL phase. Here the mixed phase is determined by Gibbs phase rules and the global conservation law for baryon number. The Gibbs conditions read

$$P^h = P^q , \quad (29)$$

$$\mu_n = 3\mu , \quad (30)$$

where μ_n and μ are neutron and quark chemical potential. The global baryon number conservation law is imposed through the relation

$$n_b = (1 - \chi)n_b^h + \chi n_b^q , \quad (31)$$

where χ is the volume fraction of the CFL phase in the mixed phase and n_b^h and n_b^q are baryon densities in the hadronic and CFL phase respectively. The total energy density in the mixed phase is

$$\epsilon = (1 - \chi)\epsilon^h + \chi\epsilon^q . \quad (32)$$

III. RESULTS AND DISCUSSIONS

In the DDRH model, the dependence of meson-nucleon vertices on total baryon density is obtained from microscopic Dirac-Brueckner calculations of symmetric and asymmetric matter using Groningen nucleon-nucleon potential [38–40]. We adopt a suitable parameterisation for density dependent couplings as was given by Ref. [32]. The density dependent meson-nucleon couplings at saturation density are listed in Table I of Ref. [13]. The saturation properties calculated using these couplings are binding energy $E/A = -15.6$ MeV, saturation density $n_0 = 0.18 fm^{-3}$, symmetry energy coefficient $a_{sym} = 26.1$ MeV and incompressibility $K = 282$ MeV [13].

The density dependence of meson-hyperon vertices are obtained from density dependent meson-nucleon couplings using hypernuclear data [8] and scaling law [41]. The ratio of meson-hyperon coupling to meson-nucleon coupling for Groningen potential is given by Table II of Ref. [13]. Similarly, we employ the density independent meson-(anti)kaon couplings of Ref. [13] in our calculation.

Now we report the results of our calculation. In the CFL phase, we have neglected the density dependence of strange quark mass (m_s) and color superconducting gap (Δ). We discuss here first order nuclear matter to CFL quark matter phase transition for different values of gap and strange quark mass whereas the bag constant is fixed at $B^{\frac{1}{4}} = 180$ MeV. We also show the results of hadronic to unpaired ($\Delta = 0$) quark matter phase transition. Nuclear matter is composed of neutrons, protons, electrons and muons whereas the CFL phase contains paired quarks and K^0 condensate. For hadronic to unpaired quark matter phase transition, we have imposed both global baryon and electric charge conservation in the mixed phase. On the other hand, we have global baryon number conservation and local color and charge neutrality in the mixed phase of nuclear-CFL phase transition. The lower and upper boundary of the mixed phase for different values of Δ and m_s and $B^{\frac{1}{4}} = 180$ MeV are recorded in Table I. Here we note that the phase transition to CFL quark matter is delayed to higher densities for a larger value of m_s . On the other hand, the phase transition occurs earlier for case $\Delta = 100$ MeV than that of case $\Delta = 57$ MeV irrespective of strange quark mass. We also note that the extent of the mixed phase involving unpaired quark matter is the largest among all the cases studied here. The average quark chemical potential at the onset of the phase transition is shown in Table I. We find that the CFL phase is energetically favoured over unpaired quark matter because $\Delta > m_s^2/4\mu$ is satisfied [25].

Pressure versus energy density and gravitational mass against central energy density for different values of gap ($\Delta = 0, 57$ and 100 MeV) and $m_s = 150$ and 200 MeV and $B^{1/4} = 180$ MeV are exhibited in Fig. 1 and Fig. 2 respectively. The static structures of spherically symmetric neutron stars calculated using Tolman-Oppenheimer-Volkoff (TOV) equations and the equations of state are presented in Fig. 2. We adopt Negele and Vautherin [42] and Baym-Pethick-Sutherland [43] equations of state to describe nuclear matter at very low density. For unpaired quark matter and paired quark matter with $\Delta = 57$ MeV, the overall EoS with $m_s = 200$ MeV is stiffer than that of $m_s = 150$ MeV. Consequently, the compact star in the former case has a larger maximum mass than that of the latter case. The effect of m_s is most pronounced for unpaired quark matter. However, for $\Delta = 100$ MeV and different values of m_s there is no significant change in the EoS and maximum star masses. Again, we find the maximum masses for $\Delta = 57$ MeV is reduced compared with those for $\Delta = 100$ MeV because the EoS in the latter case is stiffer. Recently, Alford and Reddy [30] also investigated the influence of m_s and Δ on the EoS and structure of compact stars in nuclear-CFL quark matter phase transition using different models for the hadronic phase. Our results are in qualitative agreement with their findings. In our calculation, we do not consider the variation of bag constant on nuclear-CFL quark matter phase transition. But we expect similar qualitative feature as it was observed for the phase transition involving unpaired quark matter. It is worth mentioning here that a larger value of bag constant makes the EoS of unpaired quark matter soft delaying the phase transition to higher density [7].

The composition of β -equilibrated matter relevant to compact stars is displayed in Fig.

3. The hadronic phase is composed of n, p, Λ , Ξ and leptons. On the other hand, we have included the contribution of Goldstone boson K^0 in the CFL phase. Here, we take bag constant $B^{\frac{1}{4}} = 180$ MeV, $m_s = 150$ MeV and $\Delta = 57$ MeV to describe the CFL quark matter. The charge neutrality in the hadronic phase is maintained by protons, electrons and muons. We observe that Λ hyperons appear at $1.99n_0$, where $n_0 = 0.18 \text{ fm}^{-3}$. The phase transition from hadronic to CFL quark matter sets in at $2.27n_0$. The early appearance of hyperons delays the phase transition to higher density compared with that of nuclear-CFL phase transition. The mixed phase is over at $3.97n_0$. It is noted here that negatively charged Ξ hyperons appear just before the onset of mixed phase at $2.26n_0$. Also, neutral K^0 condensation occurs with the onset of CFL phase and it rises rapidly. For other values of Δ and $B^{\frac{1}{4}}$, the phase boundaries are given by Table II.

Besides hyperons, we also investigate the role of K^- condensation in the hadronic phase on the composition of neutron star matter. In a recent calculation using DDRH model, it has been shown that K^- condensation in hadronic matter is a second order phase transition [13]. In Fig. 4 we exhibit the particle abundances in β -equilibrated matter including K^- condensate. The antikaon optical potential used for this calculation is $U_{\bar{K}}(n_0) = -180$ MeV and bag constant, strange quark mass and gap are 180, 150 and 57 MeV respectively. Here we find that the mixed phase begins at the same density point i.e. $2.27n_0$ as it is noted in Fig. 3. Before the onset of K^- condensate, the charge neutrality is maintained by protons and leptons. The condensation of K^- mesons occurs in the mixed phase at $2.68n_0$. As soon as K^- condensate appears, it rapidly replaces electrons and muons and grows fast. Consequently, proton density increases. Also, we observe that negatively charged Ξ hyperon disappears almost as soon as it appears. There is no influence of K^- condensate on the extent of the mixed phase because K^- condensate appears in the mixed phase. The lower and upper boundary of the mixed phase for different cases are given by Table II.

Equations of state (pressure versus energy density) for β -equilibrated compact star matter are plotted in Fig. 5. The curves correspond to calculations for different compositions with $m_s = 150$ MeV and different values of bag constant and gap. The dashed line stands for the EoS of nucleons-only matter whereas the other lines represent those of hyperon matter for different parameter sets. For $B^{\frac{1}{4}} = 180$ MeV and $\Delta = 57$ MeV, the EoS for hyperon matter is slightly softer compared with the corresponding EoS for nucleons-only matter. As the bag constant is increased keeping the gap fixed, we find the corresponding equations of state become stiffer. The stiffer EoS among all cases considered here corresponds to the EoS for hyperon matter with $\Delta = 30$ MeV.

The maximum neutron star masses (M_{max}/M_{solar}) and their central densities ($u_{cent} = n_{cent}/n_0$) for various compositions of matter and parameter sets are listed in Table II. The static neutron star sequences representing the stellar masses M/M_{solar} and the corresponding central energy densities (ε_c) for different values of bag constant and gap are shown in Fig. 6. The closed circle on each curve denotes the maximum mass star. For $B^{\frac{1}{4}} = 180$ MeV and $\Delta = 57$ MeV, the maximum mass of nucleons-only star is $1.500M_{solar}$ corresponding to central energy density $717.46 \text{ MeV}/\text{fm}^3$, whereas that of hyperon star is $1.477M_{solar}$ corresponding to $\varepsilon_c = 717.47 \text{ MeV}/\text{fm}^3$. The maximum mass of the star including hyperons is smaller than that of the nucleons-only star because the EoS is softer in former case. The maximum masses of compact stars increase as we increase the bag constant or decrease the gap. This is evident from Fig. 6 and Table II. We also note from Table II that the

central densities corresponding to maximum neutron star masses fall in the mixed phase. So maximum mass neutron stars are hybrid star here. For each of the bottom three curves we find an unstable region followed by a stable sequence of superdense stars beyond the neutron star branch. The stable branch of superdense stars beyond the neutron star branch is called the third family branch [12,15,44–46]. It was earlier shown by various authors that the compact stars in the third family branch had different compositions and smaller radii than those of the neutron star branch. In this calculation, the superdense stars in the third family branch may contain a pure CFL quark matter core because those stars appear after the mixed phase is over.

We also calculate the EoS and structure of compact stars in the phase transition from hadronic matter including K^- condensate to CFL quark matter. Equations of state and compact star mass sequences are plotted in Fig. 7 and Fig. 8 respectively for various compositions and parameter sets. The phase boundaries and maximum neutron star masses with their central densities are given by Table II. The dashed line corresponds to the nucleons-only case whereas the other curves represent hyperon systems in both the figures. For all cases studied here, we find that K^- condensation occurs in the mixed phase.

In Fig. 8 we find that the static neutron star sequence including hyperons and K^- condensate and calculated with $B^{\frac{1}{4}} = 180$ MeV, $\Delta = 57$ MeV, $m_s = 150$ MeV and $U_{\bar{K}}(n_0) = -180$ MeV has a lower maximum mass $1.464M_{solar}$ corresponding to central energy density $\varepsilon_c = 690.19$ MeV/fm³ than the corresponding nucleons-only star of $1.503M_{solar}$ corresponding to central energy density $\varepsilon_c = 689.59$ MeV/fm³. This may be attributed to the fact that the EoS in the former case is softer than that of the latter case as it is evident from Fig. 7. In both the cases, we find third family solutions beyond neutron star branches. Here superdense stars in the third family also contain a pure CFL quark matter core. For the other case studied with $B^{\frac{1}{4}} = 185$ MeV, $\Delta = 57$ MeV, $m_s = 150$ MeV and $U_{\bar{K}}(n_0) = -160$ MeV, we obtain a stiffer EoS resulting in a larger maximum mass star $1.582M_{solar}$ corresponding to central energy density $\varepsilon_c = 803.32$ MeV/fm³.

The mass-radius relationship for nucleons-only and hyperon stars with and without K^- condensate for $B^{\frac{1}{4}} = 180$ MeV, $\Delta = 57$ MeV, $m_s = 150$ MeV and $U_{\bar{K}}(n_0) = -180$ MeV are shown in Fig. 9. The filled circles, squares and triangles correspond to maximum masses on the neutron star and third family branch. The maximum masses and radii of nucleons-only stars without K^- condensate (dotted line) in the neutron star (third family) branch are $1.500(1.506)M_{solar}$ and $12.37(10.15)$ km respectively. Further inclusion of K^- condensate in nucleons-only stars does not change maximum masses as it is evident from Table II. The maximum masses and their corresponding radii for hyperon stars involving K^- condensate (solid line) in the neutron star (third family) branch are $1.464(1.492)M_{solar}$ and $12.34(9.97)$ km whereas those without K^- condensate (dashed line) are $1.477(1.498)M_{solar}$ and $12.33(10.05)$ km respectively. Both the neutron star and third family branch have smaller masses including K^- condensate than those without K^- condensate because the EoS are softer in the former case. It is interesting to note that the radii in the third family branch are smaller than their counterparts in the neutron star branch. Also, the stars in the third family branch have different compositions than those of the neutron star branch. We find mass-radius relationships discussed here are in good agreement with the observations of Cottam et al. [4]. Also, we note that compact stars constructed here do not have radii ~ 8 km or less. However, we find that compact stars including exotic phases are compatible

with the results of Ref. [3].

IV. SUMMARY AND CONCLUSIONS

We have investigated first order phase transitions from hadronic matter including hyperons and antikaon condensate to color-flavor-locked quark matter including the condensate of Goldstone boson K^0 . The DDRH model has been adopted here to describe the hadronic phase. This model takes into account many body correlations in hadronic phase by density dependent meson-baryon couplings. Density dependent meson-baryon couplings are obtained from microscopic Dirac-Brueckner calculations using Groningen nucleon-nucleon potential. In this calculation meson-(anti)kaon couplings are density independent. Here K^- condensation is found to be a second order phase transition. On the other hand, the CFL quark matter is described by the thermodynamic potential of Ref. [24]. The role of strange quark mass and color-superconducting gap on the nuclear-CFL+ K^0 matter phase transition has been studied for a fixed value of bag constant $B^{\frac{1}{4}} = 180$ MeV. The phase transition is delayed to higher density for a larger value of m_s . On the other hand, the phase transition sets in earlier as the value of gap increases. Also, we have found the early appearance of hyperons shifts the phase transition to higher density. However, K^- condensate is formed in the hadronic phase of the mixed phase and has little effect on the phase transition.

Equations of state for nuclear matter-CFL+ K^0 matter phase transition have been studied here for different values of m_s and Δ and for a fixed value of bag constant. For a fixed value of gap, the EoS becomes stiffer in case of a larger value of m_s resulting in larger maximum mass star. For a large value of gap such as $\Delta = 100$ MeV, we find that different values of strange quark mass have no impact on the EoS and the maximum masses of compact stars. Similarly, a smaller value of gap softens the EoS leading to a smaller maximum mass star. We have also constructed equations of state including hyperons and K^- condensate in the hadronic phase for different values of bag constant, gap, antikaon optical potential and $m_s=150$ MeV. The EoS including hyperons and/or K^- condensate is softer than that of nucleons-only matter. Consequently, the maximum star masses are smaller in the former cases. It is worth mentioning here that we have obtained stable branches of superdense stars called third family branches beyond neutron star branches for certain combinations of parameters. Superdense stars in the third family branch contain a pure CFL quark matter core whereas maximum mass neutron stars are hybrid stars. The compact stars in the third family have smaller radii and different compositions than those of the neutron star branch.

In this calculation, we do not consider the density dependence of strange quark mass and gap. Therefore, it would be interesting to investigate how density dependent strange quark mass and gap in the Nambu-Jona-Lasinio model [26] modify our results.

REFERENCES

- [1] J.A. Pons, F.M. Walter, J.M. Lattimer, M. Prakash, R. Neuhäuser and P. An, *Astrophys. J* **564**, 981 (2002).
- [2] J.J. Drake et al., *Astrophysics J.* **572**, 996 (2002).
- [3] F.M. Walter and J.M. Lattimer, *Astrophys. J* **564**, 981 (2002).
- [4] J. Cottam, F. Paerels and M. Mendez, *Nature* **420**, 51 (2002);
C. Miller, *Nature* **420**, 31
- [5] N. K. Glendenning, *Compact stars*, (Springer, New York, 1997).
- [6] D.B. Kaplan and A.E. Nelson, *Phys. Lett. B* **175**, 57 (1986);
A.E. Nelson and D.B. Kaplan, *Phys. Lett. B* **192**, 193 (1987).
- [7] M. Prakash, I. Bombaci, M. Prakash, Paul J. Ellis, J. M. Lattimer and R. Knorren, *Phys. Rep.* **280**, 1 (1997).
- [8] J. Schaffner and I.N. Mishustin, *Phys. Rev. C* **53**, 1416 (1996).
- [9] N.K. Glendenning and J. Schaffner-Bielich, *Phys. Rev. Lett.* **81**, 4564 (1998).
- [10] S. Pal, D. Bandyopadhyay and W. Greiner, *Nucl. Phys.* **A674**, 553 (2000).
- [11] S. Banik and D. Bandyopadhyay, *Phys. Rev. C* **63**, 035802 (2001).
- [12] S. Banik and D. Bandyopadhyay, *Phys. Rev. C* **64**, 055805 (2001).
- [13] S. Banik and D. Bandyopadhyay, *Phys. Rev. C* **66**, 065801 (2002).
- [14] E. Farhi and R.L. Jaffe, *Phys. Rev. D* **30**, 2379 (1984).
- [15] K. Schertler, C. Greiner, J. Schaffner-Bielich and M.H. Thoma *Nucl. Phys.* **A677**, 463 (2000).
- [16] J. M. Lattimer and M. Prakash, *Astrophys. J* **550**, 426 (2001) .
- [17] B.C. Barrois, *Nucl. Phys.* **B129**, 390 (1977).
- [18] S. Frautschi, *Proceedings of workshop on hadronic matter at extreme density*, Erice, 1978.
- [19] D. Bailin and A. Love, *Phys. Rep.* **107**, 325 (1984).
- [20] M. Alford, K. Rajagopal and F. Wilczek, *Phys. Lett. B* **422**, 247 (1998).
- [21] R. Rapp, T. Schäfer, E.V. Shuryak and M. Velkovsky, *Phys. Rev. Lett.* **81**, 53 (1998).
- [22] M. Alford, K. Rajagopal and F. Wilczek, *Nucl. Phys.* **B537**, 443 (1999).
- [23] D.H. Rischke and R.D. Pisarski, *nucl-th/0004016*.
- [24] K. Rajagopal and F. Wilczek, *Handbook of QCD*, Edited by M. Shifman (World Scientific, Singapore, 2001).
- [25] M. Alford and K. Rajagopal, *JHEP* **06**, 031 (2002).
- [26] A. Steiner, S. Reddy and M. Prakash, *Phys. Rev. D* **66**, 094007 (2002).
- [27] D.B. Kaplan and S. Reddy, *Phys. Rev. D* **65**, 054042 (2001).
- [28] P.F. Bedaque and T. Schäfer, *Nucl. Phys.* **A677**, 802 (2002).
- [29] M. Alford, K. Rajagopal, S. Reddy and F. Wilczek, *Phys. Rev. D* **64**, 074017 (2001).
- [30] M. Alford and S. Reddy, *nucl-th/0211046*.
- [31] G. Lugones and J. E. Horvath, *astro-ph/0211638*.
- [32] F. Hofmann, C.M. Keil and H. Lenske, *Phys. Rev. C* **64**, 034314 (2001).
- [33] F. Hofmann, C.M. Keil and H. Lenske, *Phys. Rev. C* **64**, 025804 (2001).
- [34] C. Fuchs, H. Lenske and H.H. Wolter, *Phys. Rev. C* **52**, 3043 (1995).
- [35] H. Lenske and C. Fuchs, *Phys. Lett. B* **345**, 355 (1995).
- [36] J. Madsen, *Phys. Rev. Lett.* **87**, 172003 (2001).
- [37] N.K. Glendenning, *Phys. Rev. D* **46**, 1274 (1992).

- [38] F. de Jong and H. Lenske, Phys. Rev. C **57**, 3099 (1998).
- [39] F. de Jong and H. Lenske, Phys. Rev. C **58**, 890 (1998).
- [40] R. Malfliet, Prog. Part. Nucl. Phys. **21**, 207 (1988).
- [41] C.M. Keil, F. Hofmann and H. Lenske, Phys. Rev. C **61**, 064309 (2001).
- [42] J.W. Negele and D. Vautherin, Nucl. Phys. **A207**, 298 (1974).
- [43] G. Baym, C.J. Pethick and P. Sutherland, Astrophys. J. **170**, 299 (1971).
- [44] U.H. Gerlach, Phys. Rev. **172**, 1325 (1968).
- [45] N. K. Glendenning and C. Kettner, Astron. Astrophys. **353**, L9 (2000).
- [46] J. Schaffner-Bielich, M. Hanauske, H. Stöcker and W. Greiner, Phys. Rev. Lett. **89**, 171101 (2002).

TABLES

TABLE I. Lower(u_l) and upper(u_u) boundary of the mixed phase in nuclear-CFL phase transition for different values of gap $\Delta = 0$ (unpaired quark matter), 57, 100 MeV and strange quark mass $m_s = 150$ and 200 MeV for a given value of bag constant $B^{\frac{1}{4}} = 180$ MeV. Here $u = n_B/n_0$ and saturation density is $n_0 = 0.18 fm^{-3}$. Average quark chemical potential at the onset of phase transition is also given here.

$B^{\frac{1}{4}}$ (MeV)	m_s (MeV)	Δ (MeV)	μ (MeV)	u_l	u_u
180	150	0	360.03	1.90	5.33
180	"	57	374.65	2.14	3.97
180	"	100	336.07	1.43	3.09
180	200	0	375.06	2.14	5.77
180	"	57	480.74	3.57	4.61
180	"	100	352.08	1.76	3.36

TABLE II. The maximum neutron star masses M_{max} and their corresponding central densities $u_{cent}=n_{cent}/n_0$ with different compositions in a first order hadronic to CFL quark matter phase transition. The lower (u_l) and upper(u_u) boundary of the mixed phase and the threshold density of K^- condensation in hadronic phase $u_{th}^{K^-}$, where $u = n_B/n_0$, for antikaon optical potential depth $U_{\bar{K}}(n_0)$ MeV at saturation density $n_0 = 0.18fm^{-3}$ are given for various values of bag constant $B^{\frac{1}{4}}$ and gap Δ .

	$B^{\frac{1}{4}}$ (MeV)	Δ (MeV)	$U_{\bar{K}}(n_0)$ (MeV)	CFL		$u_{th}^{K^-}$	u_c	$\frac{M_{max}}{M_{solar}}$
				u_l	u_u			
np \rightarrow CFL+ K^0	180	57		2.14	3.97		3.97	1.500
np $\Lambda\Xi \rightarrow$ CFL+ K^0	180	57		2.27	3.97		3.97	1.477
do	182	57		2.60	4.20		4.06	1.530
do	184	57		3.02	4.48		4.06	1.569
do	180	30		3.14	4.43		4.07	1.578
np $K^- \rightarrow$ CFL+ K^0	180	57	-180	2.14	3.97	2.36	3.82	1.503
np $\Lambda\Xi K^- \rightarrow$ CFL+ K^0	180	57	-180	2.27	3.94	2.68	3.82	1.464
do	185	57	-160	3.28	4.63	3.20	4.27	1.582

FIGURES

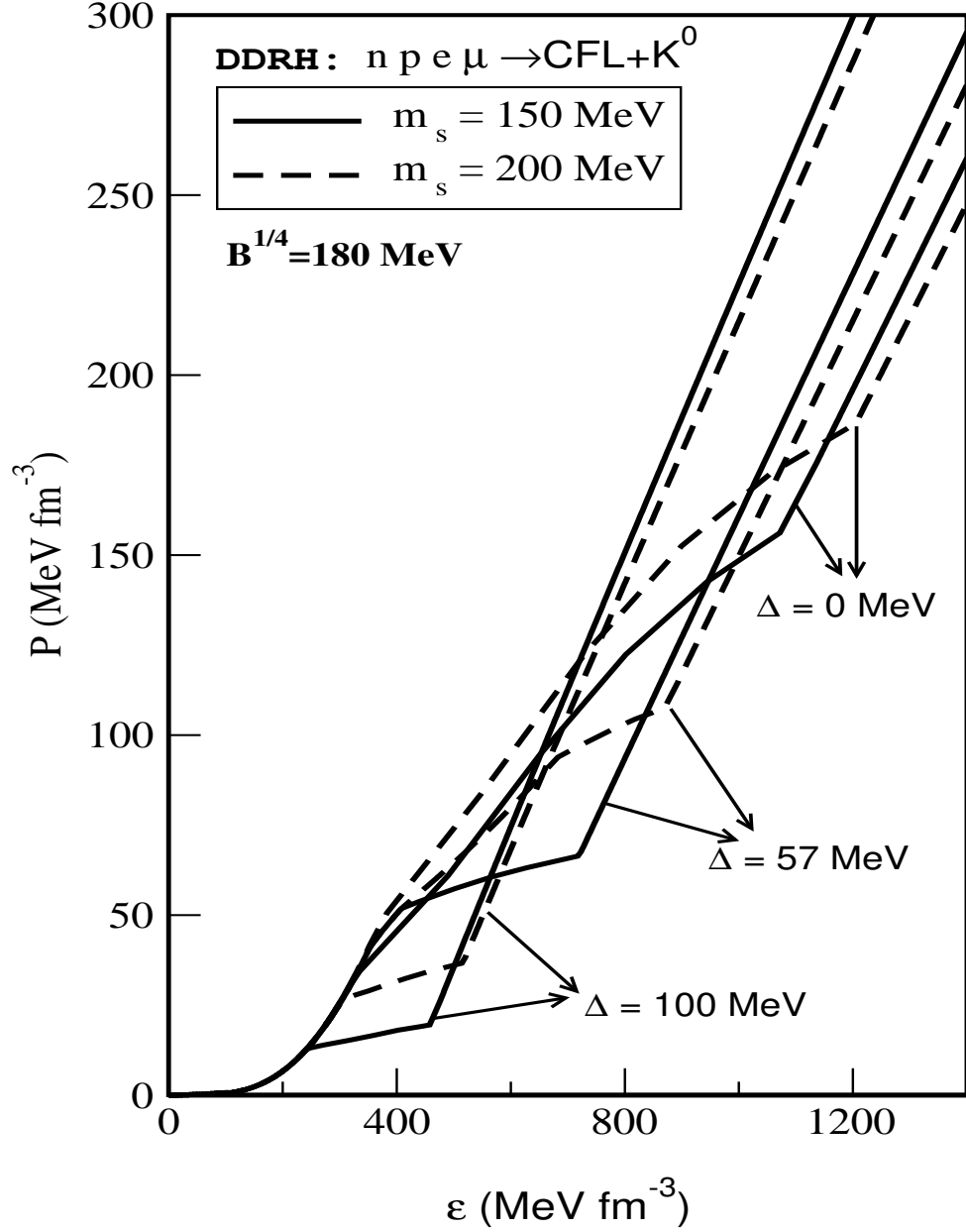


FIG. 1. The equations of state, pressure P versus energy density ϵ for n , p , lepton and CFL quark matter including K^0 condensate with $B^{1/4} = 180 \text{ MeV}$ and different values of $\Delta=0$ (unpaired quark matter), 57 MeV and 100 MeV and $m_s = 150 \text{ MeV}$ and 200 MeV are compared.

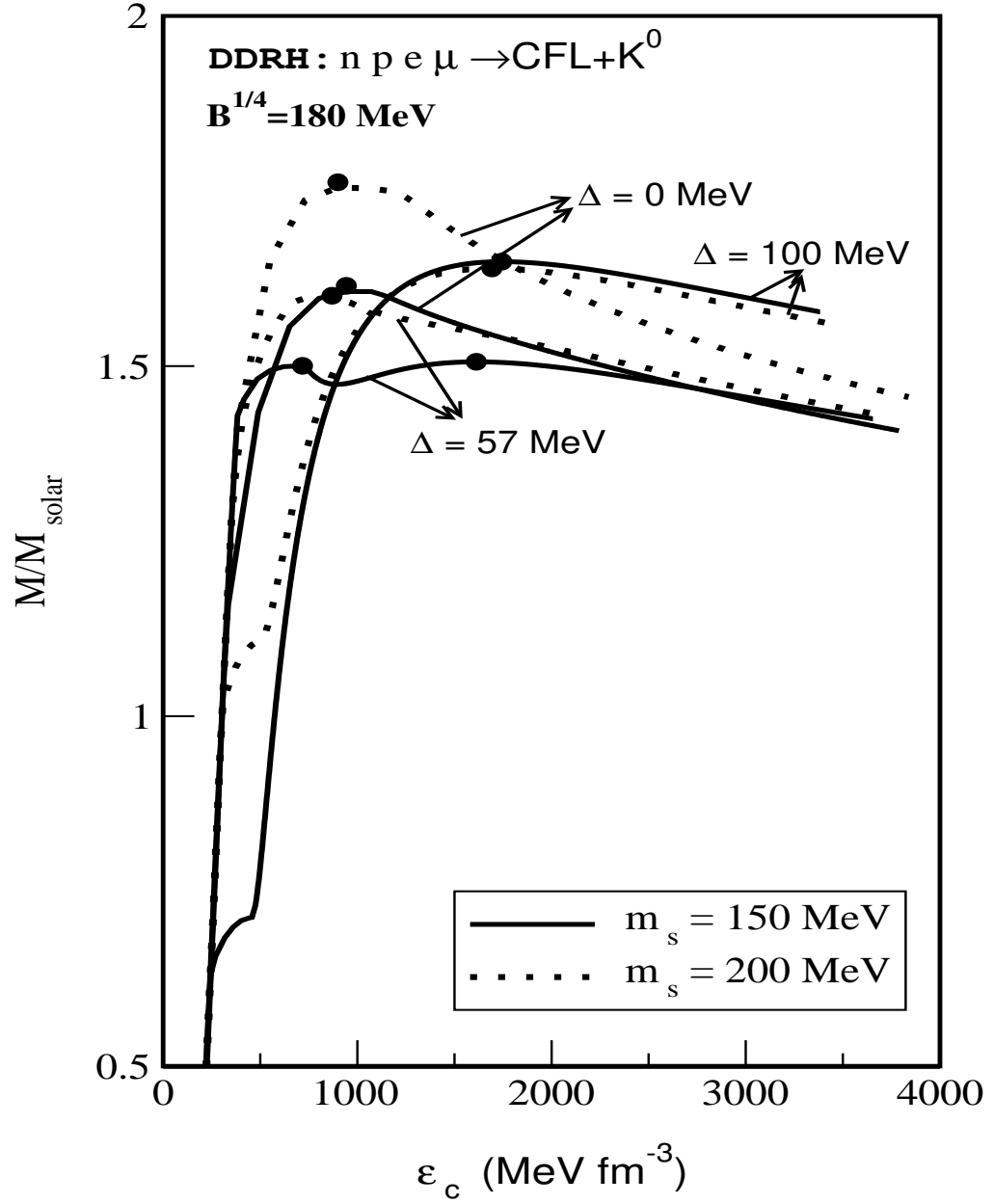


FIG. 2. The corresponding mass sequences for EoS of Fig. 1 are plotted .

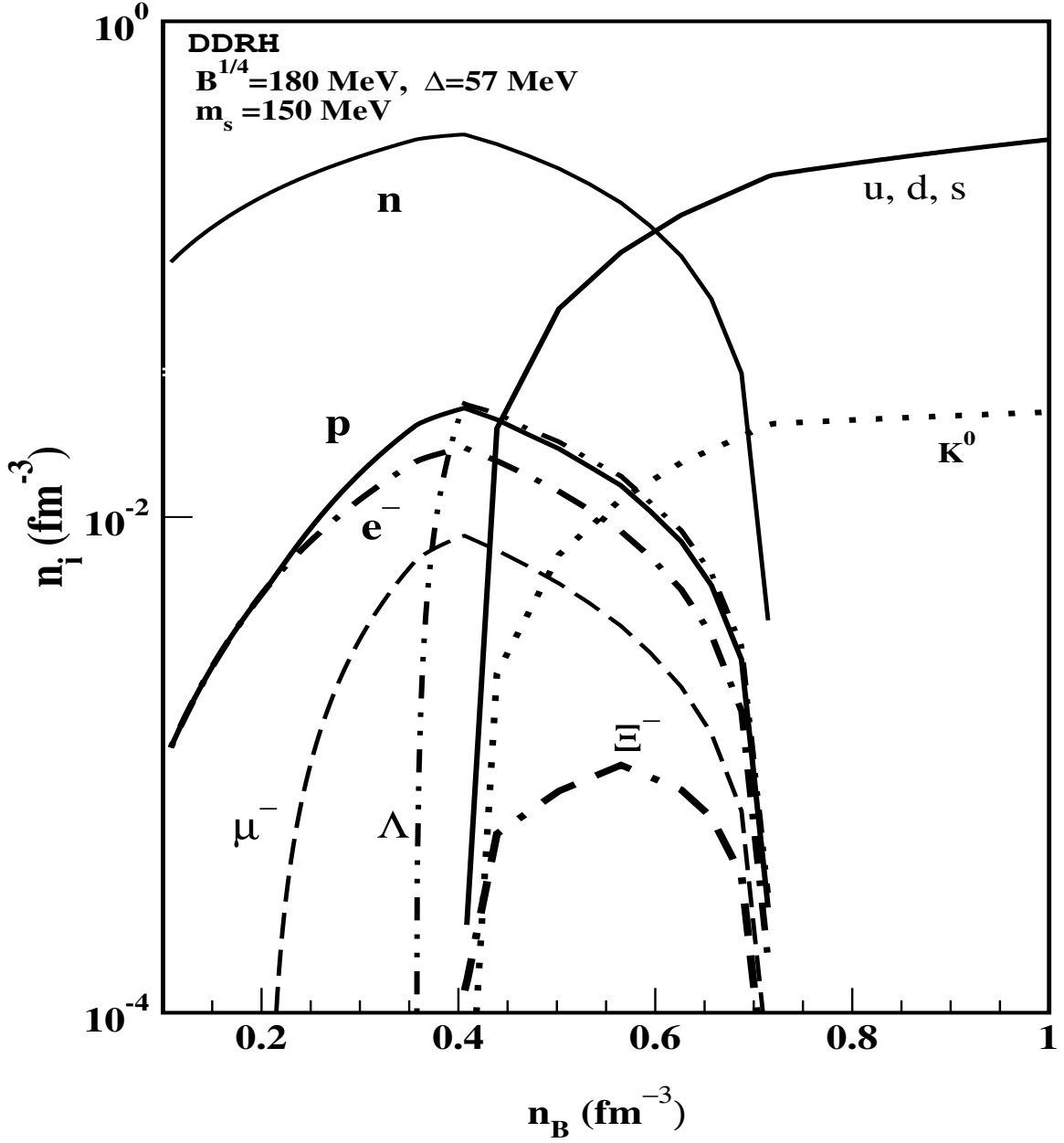


FIG. 3. Number densities (n_i) of various particles in β -equilibrated n, p, Λ , Ξ , lepton and CFL+ K^0 matter for $B^{1/4} = 180 \text{ MeV}$, $\Delta = 57 \text{ MeV}$, and $m_s = 150 \text{ MeV}$ as a function of baryon density.

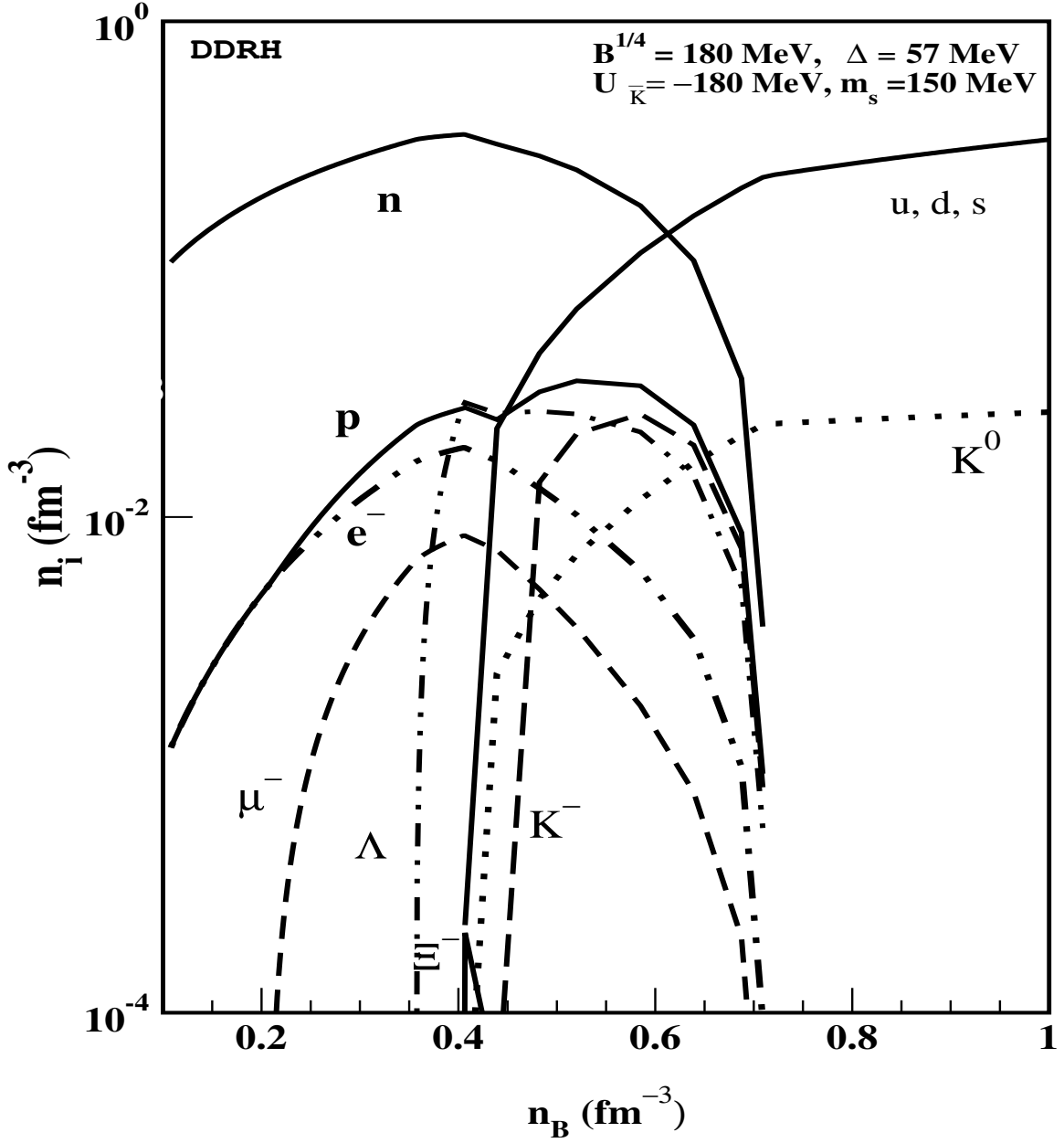


FIG. 4. Number densities (n_i) of various particles in β -equilibrated n, p, Λ , Ξ , K^- , lepton and CFL+ K^0 matter for $B^{1/4} = 180$ MeV, $\Delta = 57$ MeV, $m_s = 150$ MeV and antikaon optical potential depth $U_{\bar{K}}(n_0) = -180$ MeV at normal nuclear matter density as a function of baryon density .

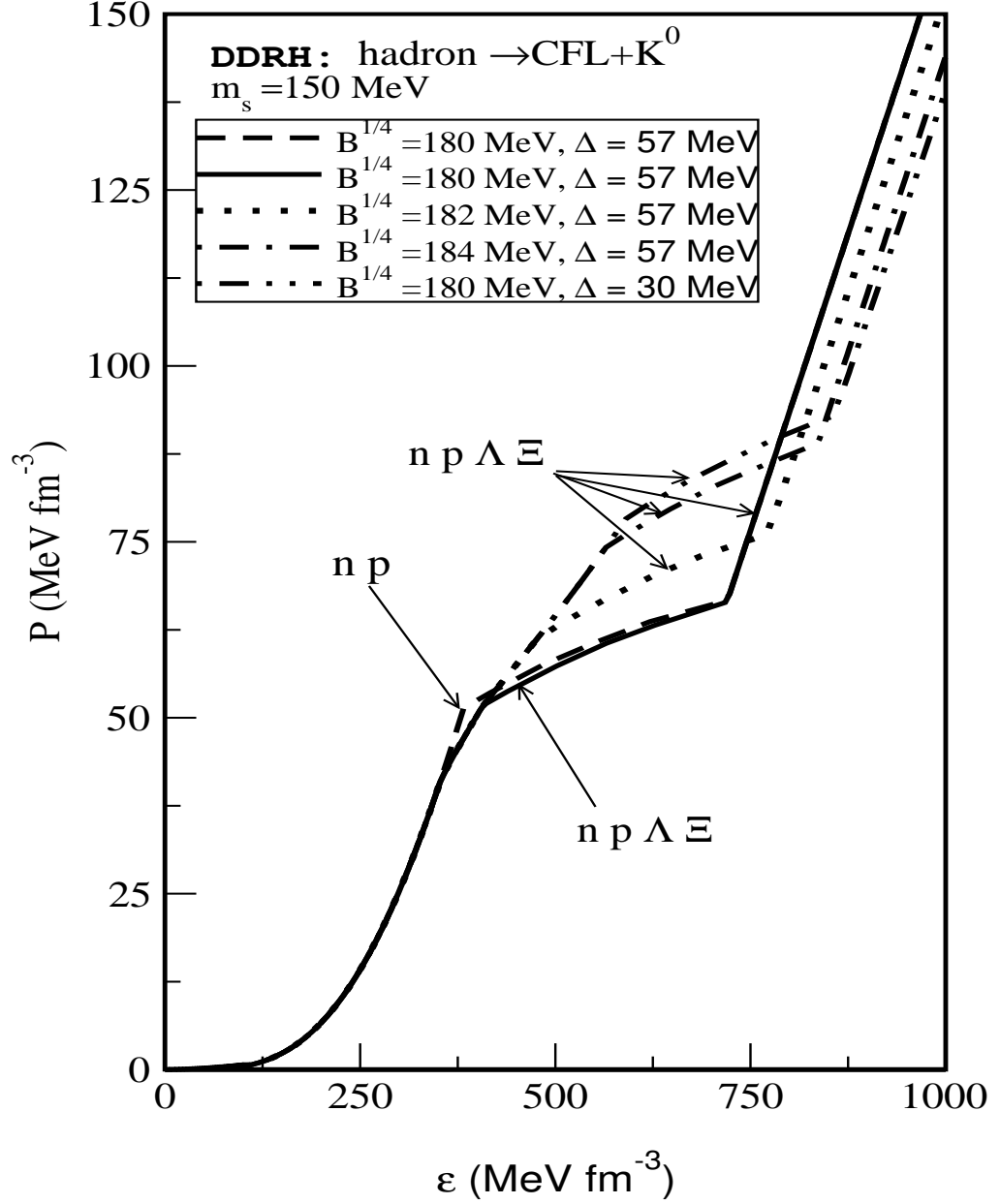


FIG. 5. The equation of state, pressure P versus energy density ε is shown here. The results are for n, p, lepton and CFL+ K^0 matter (dashed line) and n, p, Λ , Ξ , lepton and CFL+ K^0 matter (other lines) for $m_s = 150$ MeV and different values of bag constant and gap.

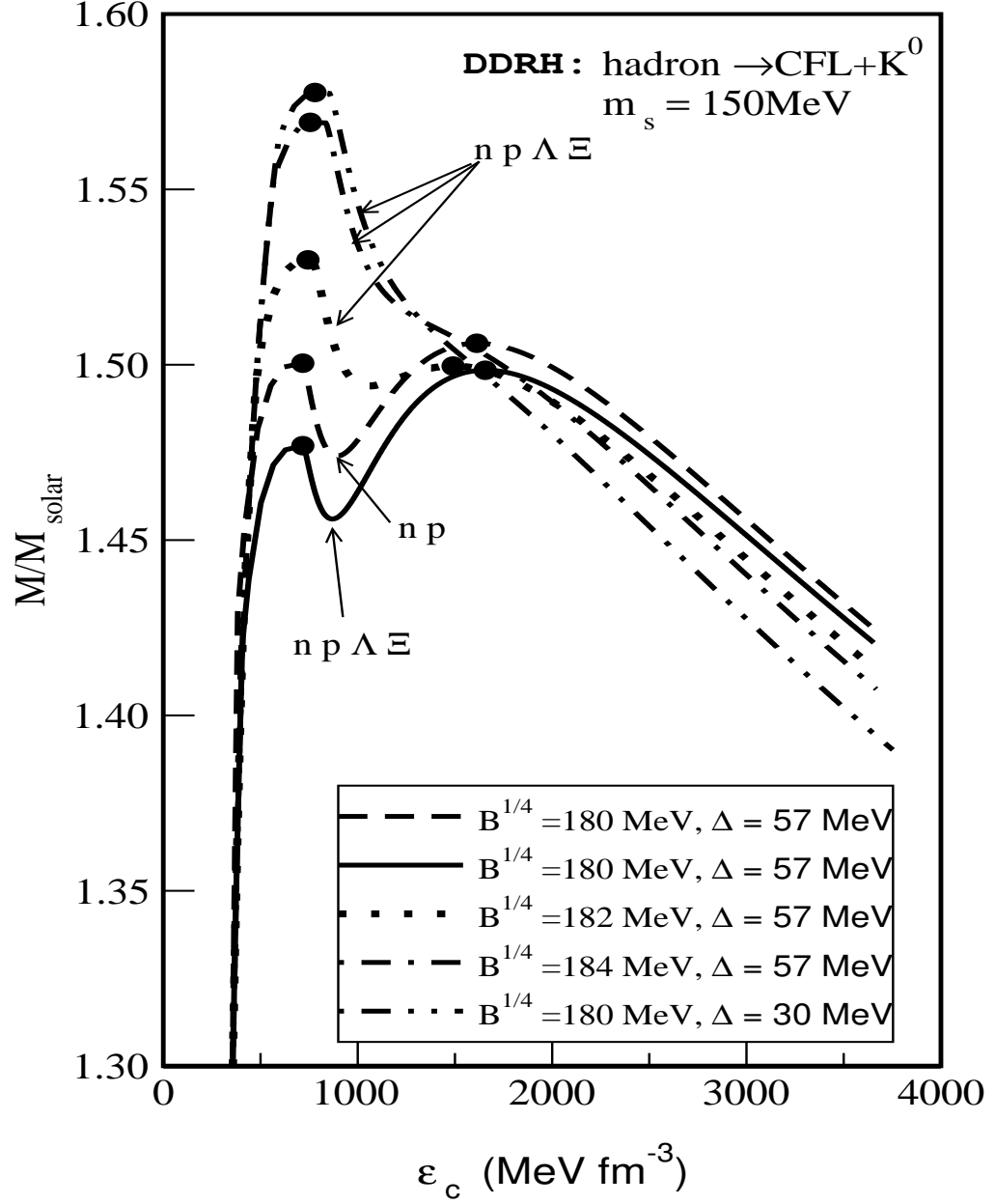


FIG. 6. The compact star mass sequences are plotted with central energy density for the corresponding EoS of Fig. 5.

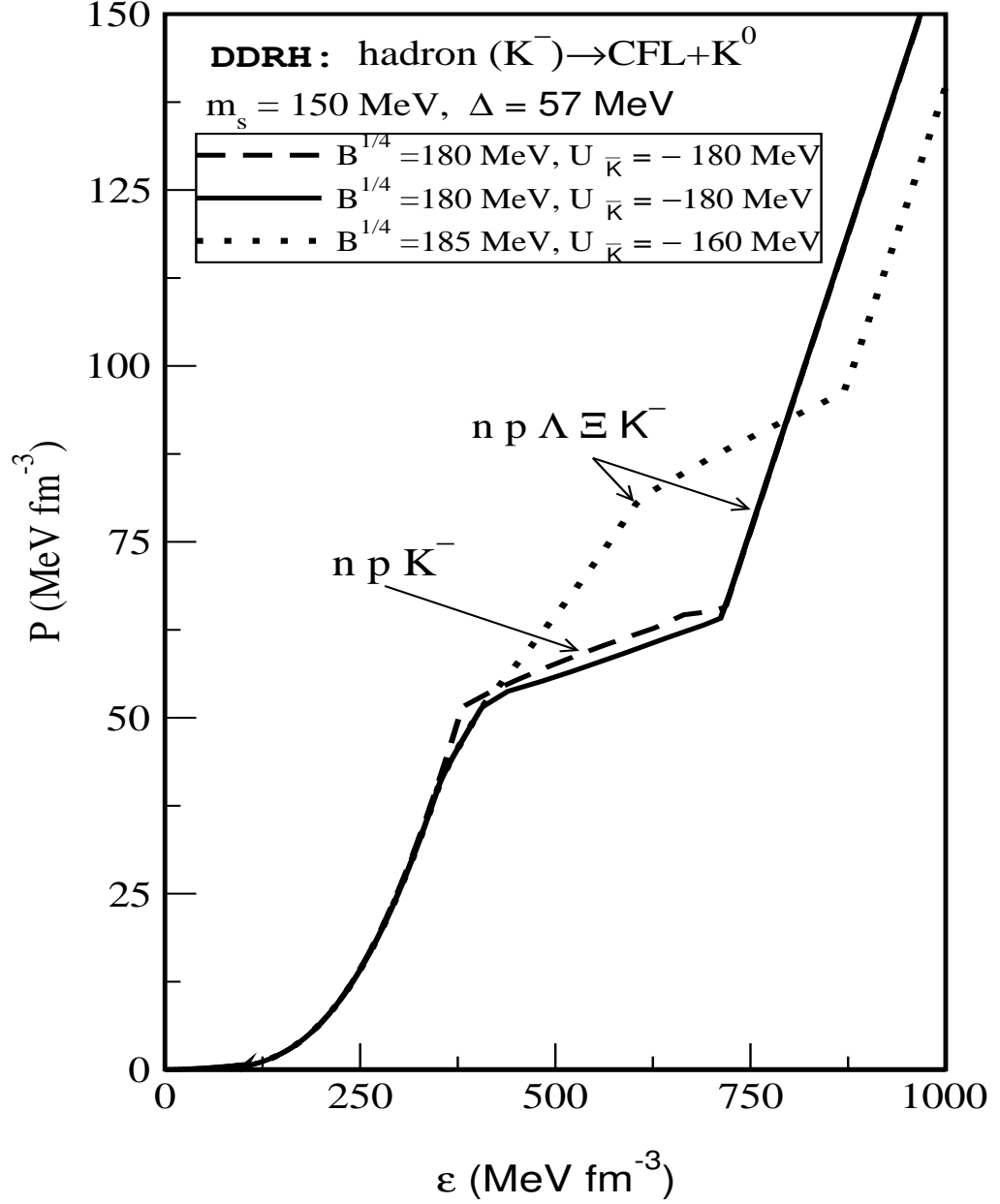


FIG. 7. The equation of state, pressure P versus energy density ε , is shown here. The results are for hadronic matter including K^- condensate and CFL+ K^0 matter for $m_s = 150$ MeV, $\Delta = 57$ MeV and different values of bag constant and antikaon optical potential depth $U_{\bar{K}}(n_0) = -160$ and -180 MeV at normal nuclear matter density.

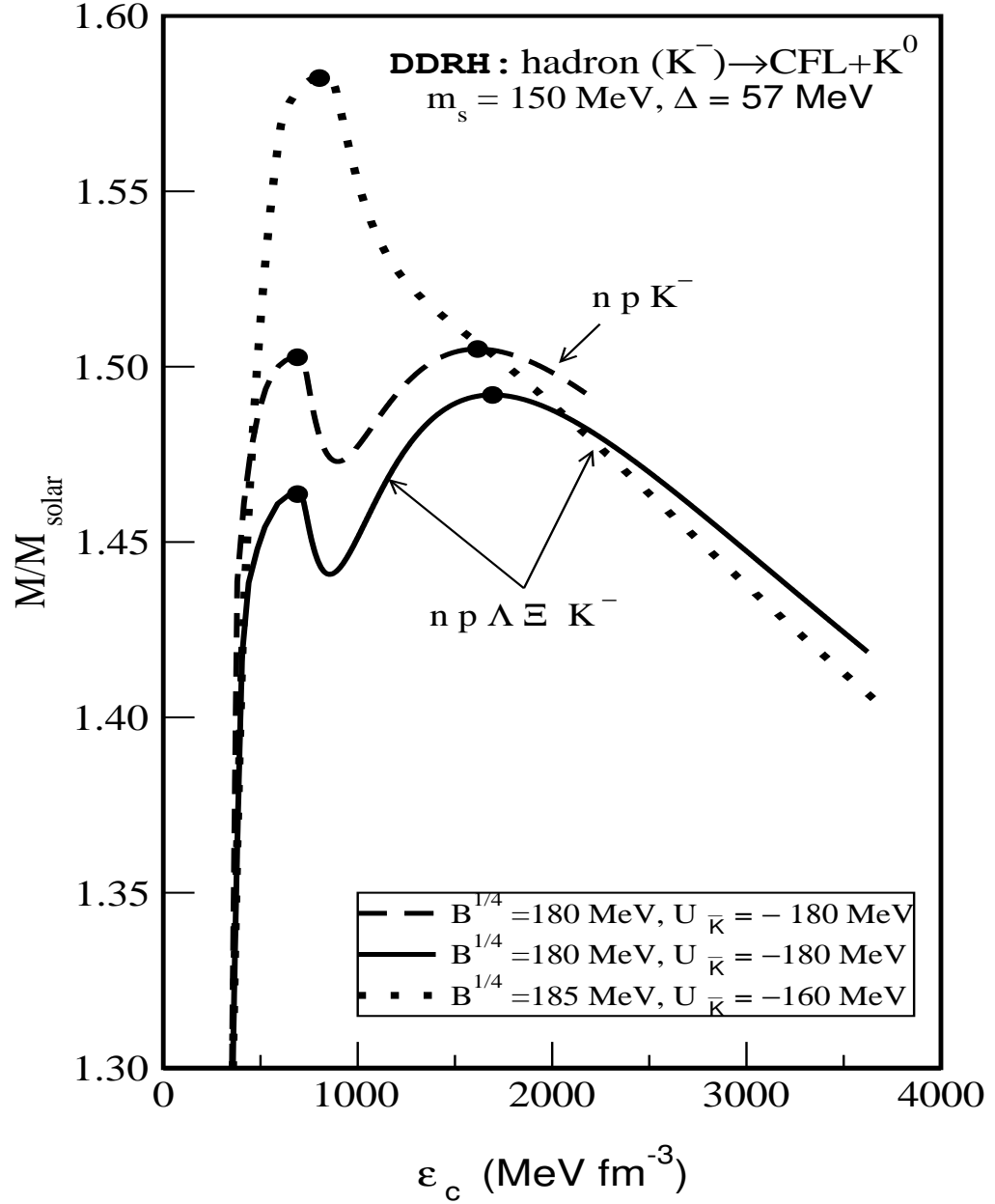


FIG. 8. The compact star mass sequences are plotted with central energy density for the corresponding EoS of Fig. 7.

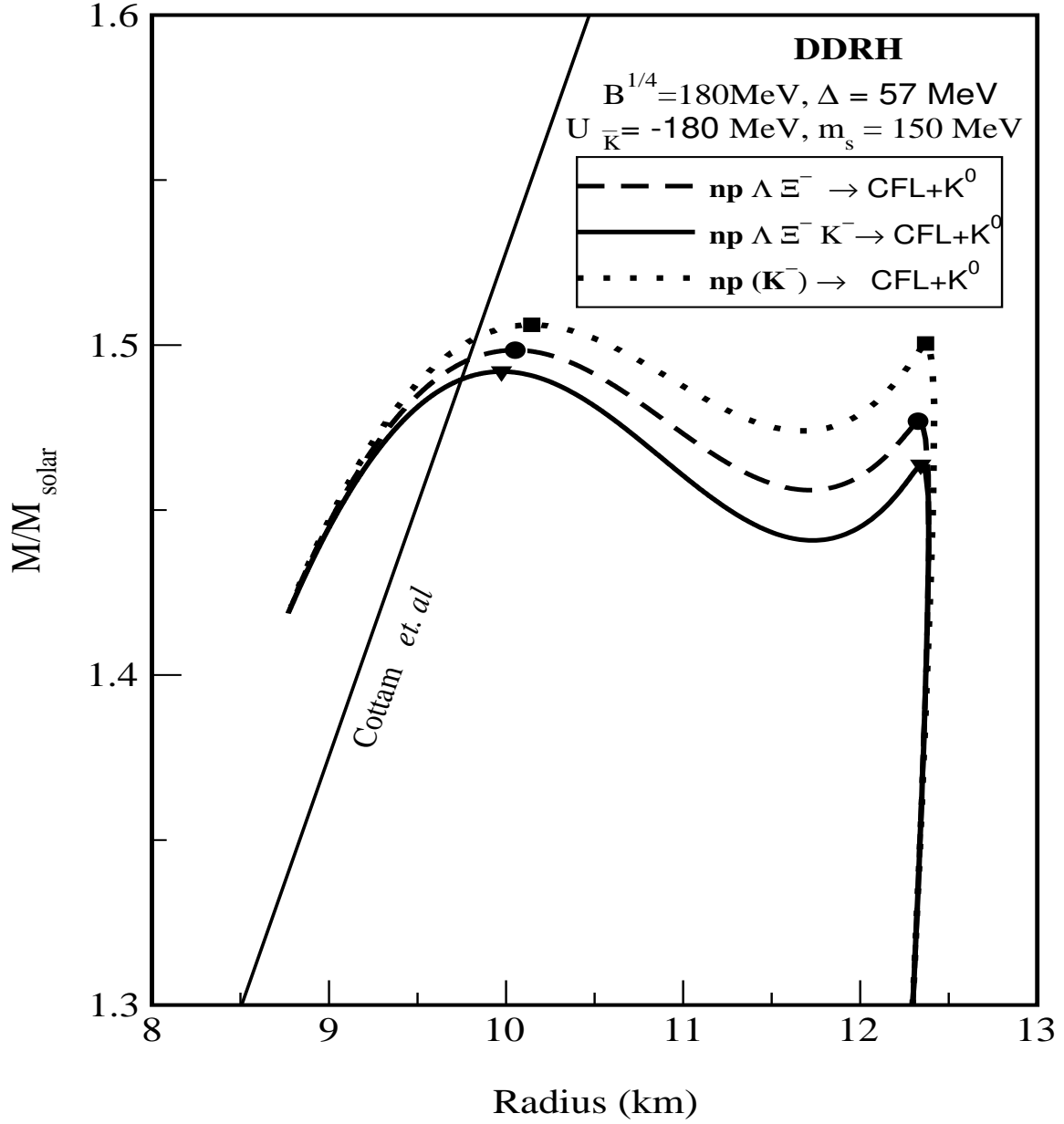


FIG. 9. The mass-radius relationship for compact star sequences for n, p, Λ , Ξ , lepton and CFL+ K^0 matter with $B^{1/4} = 180 \text{ MeV}$, $m_s = 150 \text{ MeV}$, gap=57 MeV and with K^- ($U_{\bar{K}}(n_0) = -180 \text{ MeV}$) and without K^- condensate.